

GEOSTATIONARY SATELLITE POSITION DETERMINATION FOR COMMON-VIEW TWO-WAY TIME TRANSFER MEASUREMENTS

Zhuang Qixiang and R.J. Douglas
INMS, National Research Council
Ottawa, Canada K1A 0R6

Abstract

In common-view two-way time transfer, each earth station receives an unwanted return signal from its own transmission as well as the desired signal from the other earth station. NRC, NIST and USNO have been cooperating in a three-corner common-view two-way time transfer experiment. Some systematic effects are known to depend on the position of the satellite (Sagnac effect and the cross-correlation pulling of the pseudo-random codes).

A method is presented for deriving accurate satellite ranges from each of three stations doing common-view two-way satellite time transfer measurements, when one (and only one) station also takes ranging measurements on its "unwanted return signal" for a brief period. The method is applied to determine the variations in position of the satellite used over the course of the NRC/NIST/USNO SBS-3 experiment, with ranging data taken at NRC, where no additional hardware was required to automate the process.

The fit and extrapolation which are employed in this method have an estimated precision of 2 m. If the delays of SBS-3 satellite Ku band transponder and earth station equipment were measured accurately as well as the tropospheric refractions were well modeled and corrected, we would expect a ranging accuracy of 2.5 m and satellite positioning accuracy would be 200 m (latitude) 50 m (longitude) and 20 m (height above ellipsoid).

INTRODUCTION

Two-way satellite time transfers are routinely performed between NIST and USNO, NIST and NRC, and between NRC and USNO. The first year of measurements, described here, used the SBS-3 Ku band geosynchronous satellite at 95° W. As shown in Figure 1, these three earth stations are within the -4 dB contour of the continental beam from this satellite. The earth stations are spaced on sufficiently long baselines to allow accurate satellite position determinations from ranging measurements that loop through the satellite. We have used a positioning method that adds only a little overhead to the minimal two-way time transfer when operated from one minimally equipped time-transfer earth station in a two-way time transfer network.

The set-up and all measurements are arranged to fit in a 30 minute period each Monday, Wednesday and Friday morning. As illustrated in Figure 2, three time transfer measurement groups are scheduled: *NIST(1)/USNO(0)*, *NRC(3)/NIST(4)* and *USNO(0)/NRC(1)*, each lasting 300 seconds and typically starting at 10:30, 10:37 and 10:47 respectively. A ranging measurement at NRC, *NRC(4)* which lasts 100 seconds, is inserted between *NRC(3)/NIST(4)* and *USNO(0)/NRC(1)*. For each institute, the number in brackets indicates the receiving code of the Mitrex 2500 modem's pseudorandom noise (PRN) sequence.

A method is described below for deriving accurate range data (of the satellite from the three stations) from two groups of time transfer measurements *NRC(3)/NIST(4)* and *USNO(0)/NRC(1)* as well as one station ranging *NRC(4)*. The synchronism which is required for three-station simultaneous ranging is created by means of polynomial fits and extrapolation of the time transfer data *NRC(3)*, *NIST(4)*, *NRC(1)* and *USNO(0)*. This is a “pseudo synchronism” method which exploits the slow rate change of timing (a few ns/s was typical for SBS-3) and the high precision of the timing (residuals of less than 1 ns for 1 s measurements). After extrapolation, five sets of simultaneous fits (and measurements) *NRC(4)*, *NRC'(3)*, *NIST'(4)*, *NRC'(1)* and *USNO'(0)* are available. The important differences of the equipment configuration at NRC, NIST and USNO are shown in Figure 3: note differences of earth station and time interval counter (TIC) connections.

RANGE EQUATIONS

The range equations are straightforward to write down, starting with the ranging readings at NRC (*NRC(4)*) which can be expressed

$$NRC(4) = TU(NRC) + TD(NRC) + 2R(NRC) + STR \quad (1a)$$

where *TU* and *TD* are the equipment time delays of the uplink path and downlink path at earth station, *R* is the range between earth station and satellite, and *STR* is the satellite transponder time delay. Rearranging equation (1a) gives

$$R(NRC) = [NRC(4) - TU(NRC) - TD(NRC) - STR] / 2 . \quad (1b)$$

The time transfer readings at NRC and NIST can be written respectively

$$NRC'(3) = PPSx(NIST) - dTx(NIST) + TU(NIST) + WE + TD(NRC) - PPSx(NRC) \quad (2)$$

$$NIST'(4) = PPSx(NRC) - dTx(NRC) + TU(NRC) + EW + TD(NIST) - PPSx(NIST) \quad (3)$$

where *PPSx* is the external 1pps from the master clock driving the modem; *dTx* is the modem delay between *PPSx* and *Tx*; *EW* and *WE* are the signal path up to, through and down from the satellite going from east to west and west to east; it is easy to see that

$$WE + EW = 2R(NRC) + 2R(NIST) + 2STR \quad (4)$$

Using a pair of microwave relays and a 2.3 GHz translator, the “station loop delay” at NRC, *SL*, has been measured routinely. *SL* and total station equipment delay (*TU* + *TD*) are different. From Figure 3, we have

$$SL = TU + TD - 2DH + TRL \quad (5)$$

where *DH* is the antenna time delay which includes the delay of the antenna feed and connecting waveguide and cables; *TRL* is the 2.3 GHz translator delay plus connecting cable delay.

A measurement of the NIST station equipment delay has been done[D.Howe, 1987]. The NIST experiment used a satellite transponder simulator, as illustrated in Figure 4 (1). The *SL*_(NIST) as well as the sum of the simulated *STR* and *TU*_(NIST) + *TD*_(NIST) were obtained,

$$STR + TU(NIST) + TD(NIST) = 1436 \text{ ns}$$

$$SL_{(NIST)} = 1359 \text{ ns} \quad (6)$$

The experiment at NRC used a compact mixer unit, as illustrated in Figure 4 (2). *SL*_(NRC), the sum of *TU*_(NRC) and *TD*_(NRC) as well as the difference of *TRL*_(NRC) and *2DH*_(NRC) were measured,

$$TU(NRC) + TD(NRC) = 3373.5 \text{ ns}$$

$$\begin{aligned} TRL_{(NRC)} - 2DH_{(NRC)} &= 6.6 \text{ ns} \\ SL_{(NRC)} &= 3380.1 \text{ ns} \end{aligned} \quad (7)$$

Collecting the above equations, the three range equations become

$$\begin{aligned} R_{(NRC)} &= [NRC(4) - TU_{(NRC)} - TD_{(NRC)} - 83.6 \text{ ns}] / 2 \\ &= [NRC(4) - TRL_{(NIST)} + 2DH_{(NIST)} - 3450.5 \text{ ns}] / 2 \end{aligned} \quad (8)$$

$$R_{(NIST)} = [NIST'(4) + NRC'(3) - NRC(4) + dTx_{(NRC)} + dTx_{(NIST)} - 1435.5 \text{ ns}] / 2 \quad (9)$$

$$\begin{aligned} R_{(USNO)} &= [NRC'(1) + USNO'(0) - NRC(4) + dTx'(NRC) + TU_{(NIST)} + TD_{(NIST)} - TU_{(USNO)} - TD_{(USNO)} \\ &\quad - 1435.5 \text{ ns}] / 2 \\ &= [NRC'(1) + USNO'(0) - NRC(4) + dTx'(NRC) - SL_{(USNO)} + TRL_{(USNO)} - TRL_{(NIST)} \\ &\quad + 2DH_{(NIST)} - 2DH_{(USNO)} - 77 \text{ ns}] / 2 \end{aligned} \quad (10)$$

Thus the problem reduces to knowing the sum delay of TU and TD at NIST and USNO, these delays could be measured by transporting a compact calibration unit to the NIST and USNO earth station sites.

ALGORITHM OF SATELLITE POSITION DETERMINATION

In general, it is necessary to measure at least four ranges of four observing stations for determining the position and time of a space target. The independent range variable L_i is the function of target coordinates X_s, Y_s, Z_s , observing station coordinates X_i, Y_i, Z_i and measuring time t_i

$$L_i = Y(X_s, Y_s, Z_s, X_i, Y_i, Z_i, t_i) \quad (i=1,4) \quad (11)$$

If the clocks of the observing stations have been synchronized precisely and the ranging measurements are conducted at a common time t , then only three observing stations are required for the determination of target coordinates. The weighted observing equation and the weighted least-squares solution

$$G^T W G X = G^T W (O - C) \quad (12)$$

$$X = (G^T W G)^{-1} G^T W (O - C) \quad (13)$$

where, X is target position improvement matrix; G is the measurement matrix; W is the weighting matrix; and $O - C$ is the matrix of difference between measured and computed ranges. If G is square matrix and $\det G = |G| \neq 0$, equation (13) becomes

$$X = (W G)^{-1} W (O - C) \quad (14)$$

In our case, the known numbers are the coordinates of three observing stations, the independent ranges between satellite and three stations and the initial rough position of satellite. The determination of W is based on ranging precision at each station, the weighting factor is the reciprocal of ranging precision. Due to the different antenna size of earth stations and the introduction of polynomial extrapolation and conversion equation in range determination, the ranging precisions at three stations become unequal in our case. Based on the error estimates of ranging and time transfer measurements, range conversion as well as extrapolation, the differential weighting matrix W has been established. The algorithm employed in the position determination process is a standard differential correction technique of weighted least-square that minimises the observation residuals, i.e. the difference between the measured ranges and calculated ranges. The satellite initial position is iteratively replaced by the corrected satellite position, the iterative process continues until the position converges to within a delta value of error. The covariance matrix

$$P = (G^T W G)^{-1} W \quad (15)$$

is used to determine the goodness of each solution fit to the data and is used to calculate the Position Dilution Of Precision (PDOP). PDOP is the coherent factor between the position accuracy of satellite and the geometric distribution between satellite and observing stations.

$$PDOP = \sqrt{P_{11} + P_{22} + P_{33}} \quad (16)$$

Where, P_{11} , P_{22} and P_{33} are the diagonal terms of P matrix. The individual DOPs (XDOP, YDOP, ZDOP) or (φ DOP, λ DOP, HDOP) could be derived from P_{11} , P_{22} and P_{33} in the different coordinate systems.

UNCERTAINTY DISCUSSION

The absolute accuracy of satellite position determination is dependent upon knowledge of ranging accuracy, Position Dilution of Precision as well as station position accuracy. Over the course of SBS-3 experiment, the single shot (1 s) precision of ranging measurement at NRC has been about ± 1.2 ns under normal circumstances. The "ranging" precisions of NIST and USNO through conversion (but excluding extrapolation errors - discussed below) can be estimated about ± 1.6 ns and ± 2.2 ns respectively (again for 1 s measurements). It must be emphasized that the absolute accuracy of ranging measurements are subject to many systematic errors. The uncertainties relative to position determination accuracy are discussed and estimated below for our first satellite positioning results. In many cases significant improvements in accuracy could be made with rather modest efforts.

1. Polynomial extrapolation. Figure 5 shows the measurement schedule used at NRC for evaluating the accuracy of the extrapolation. The extrapolation uncertainties have been evaluated at NRC by conducting additional timing and ranging measurements: by "eavesdropping" on the NIST/USNO time transfer and measuring (receive only) timing $NRC(1)$ and $NRC(0)$; and by a second ranging session $NRC(4)$. The uncertainties of the extrapolations were evaluated by calculating the rms residual of the observed - extrapolated results, as shown in Figure 5. For extrapolation times of less than 400 seconds, a second order polynomial regression gave the best results, with rms extrapolation residuals of less than 6.8 ns.
2. Propagation delay. No cancelling of path delay exists during ranging measurement. Both the tropospheric and ionospheric refraction effects need to be taken into account. A signal propagating through the troposphere will be absorbed and delayed due to effects of snow, rain, clouds, fog as well as oxygen and water vapour molecules. The refractive correction increases with atmospheric pressure (or partial pressures of important molecules) and increases as the satellite elevation decreases. This kind of time delay could reach to several hundred nanoseconds in the worst cases. With a suitable model of tropospheric refraction, the time delay of tropospheric refraction could be corrected to about 1%. SBS-3 satellite elevations at NRC, NIST and USNO are about 34° , 42° and 41° degrees respectively. The effect of tropospheric refraction would be about 33 ns under normal circumstances. A Ku band radio signal propagating through ionosphere will be refracted, the refractive index is mainly proportional to the electron density integrated along the path and the inverse square of the signal frequency. For a 12 and 14 GHz link, the signal delay of ranging due to ionospheric refraction can be estimated as about 2 ns.
3. Satellite transponder delay. The satellite transponder delay should be available from design and acceptance test specifications and accurate to about 1 ns. In our case, the SBS-3 transponder delay is simulated by the experiment at NIST. The time delay uncertainty between the electrical centre of the satellite transponder and the simulator value was estimated as 10 ns. This effect of this delay on position will be almost the same for the three earth stations, and to first order, will simply displace the attributed position of the electrical centre of the satellite from, say, a reference plane referred to the satellite antenna.
4. Station equipment delay. To know the time delay of earth station equipment, we can measure the sum of up path and down path delay of all station equipments or alternatively the station loop delay,

the difference of antenna delays and the difference of translator delays. Based on modern technique, these equipment delays could be measured accurate to one nanosecond, but one must pay more attention to every aspect of measurement. The station loop delay SL , the modem loop delay ML and $(SL-ML)$ delay have been automatically measured at NRC as a matter of routine. Figure 6 shows the results from April, 1990 to April, 1991. $(SL-ML)$ is the total delay of the 70 MHz IF cable, Up/Down converter, 2.3 GHz translator, Tx/Rx relay and associated cables. Most of these units are operated in outdoor conditions, and so suffered environmental effects. The $(SL-ML)$ delay with a ± 1.52 ns of rms displays more noise than the ML delay with variations of ± 0.66 ns rms. The SL and $(SL-ML)$ delays show obvious seasonal variation, and a sinusoidal function, $y = \text{asin}(2\pi ct + b)$ fits the data as shown in Figure 6 with a peak-to-peak amplitude of 3.2 ns for the station loop, and 3.8 ns for the delay of the station loop minus the modem loop. The seasonal variation of the station loop delay is expected to be dominated by the temperature coefficient of the long 70 MHz IF cables, which are outdoors and buried at a depth of less than one metre for much of the run. Figure 6 also shows a small systematic drift in the modem loop delay measurements over the one year period. The station loop delay SL also has been measured at NIST, and published for a 15 day period [D. Howe, 1987]. Direct station loop delay measurements for USNO were not available. In calculation of USNO range, an estimated value of $SL(\text{USNO})$ has been used with an uncertainty of about 50 ns. The differences of translator delay and the differences of antenna delay among NRC, NIST and USNO are ignored in our calculation, thus another error of about 20 ns has been introduced.

5. PDOP. For the geometric distribution among NRC, NIST, USNO and SBS-3, the calculated PDOP is about 80. The sensitivity coefficients of latitudinal, longitudinal and height above ellipsoid position errors with respect to range error are 77.2, 20.0, 8.8 respectively. In most applications, this kind of error magnification is the limitation of the resolution of position determination. It can be reduced only by choosing optimal geometric distribution among satellite and stations.

6. Station coordinates. Errors in station coordinates have a direct effect on satellite position. The station coordinates need to be measured as accurately as possible in a common coordinate system. For the NRC earth station, the WGS-84 coordinates of the principal GPS antenna at NRC were used as the local reference. The location of the antenna of earth station was surveyed relative to the GPS antenna, and the antenna coordinates of NRC earth station were obtained with an accuracy about 7 metres. The adopted antenna coordinates of NIST and USNO earth stations were assumed with the same level of accuracy.

7. Code pulling. The ranging measurements at NRC were normally taken with no other time transfer station transmitting, and so are not expected to have any systematic pulling of the delay-locked loop of the modem's receiver. For the timing measurement runs, two PRN codes are present at the same chip rate (2.5 MHz) and length (10,000 chips). The Mitrex PRN codes are not quite orthogonal, with cross-correlation pulling averaging about 0.7% of the main autocorrelation slope used by the delay-locked loop. Averaged over all relative PRN phases, we expect a code pulling of some 2 ns rms, if the carriers are syntonized and the two signals are matched in power. Power mismatch will reduce the code pulling for the strong signal, and increase the code pulling for the weak signal. For these runs, the as-received carriers from the three earth stations rarely match within the 2 Hz noise bandwidth of the modem, giving a large rejection of the unwanted signal, to the level where code pulling is not an issue for satellite position determination.

Based on the above discussion, the current ranging accuracy is estimated as 20 m and the absolute satellite positioning accuracy is conservatively estimated as 1.6 km. If the equipment delays were measured accurately and tropospheric refractions were well modeled, the accuracy could be improved to 2.5 m (range) and 200 m (position), and only then would be limited by the extrapolation accuracy.

SATELLITE POSITION RESULTS

The satellite position determinations from April 1990 to December 1990 are presented in Figure 7. To calculate each position, a total of five data sets must be measured successfully at three stations. All five are not always available, as evidenced by the gaps in Figure 6. Note that the satellite remains within $\pm 0.03^\circ$ of a longitude 0.05° W of its nominal position of 95° W. In the periods of most nearly continuous results, shown in Figure 8, the three satellite coordinates exhibit periodic trend every 28 days.

The monthly period is attributed to the perturbing influence of the moon's gravitational force on the geostationary satellite. The moon's perturbing acceleration on a geostationary satellite has been estimated less than about 9×10^{-6} , i.e., about 5.4 km for two days tracking arc. Due to our schedule of time transfer measurements which are performed at a nearly fixed time of a day, the influence of earth's non-sphericity perturbing force are not observed. This offers a chance to see the influence of the moon's perturbation, and presumably station-keeping such as is seen on MJD 48237, indicated by a symbol ↑ in Figure 8.

EFFECTS OF SATELLITE POSITION ON TIME TRANSFER

For each of the satellite positions that were determined, the Sagnac correction was calculated for all three links: NRC/SBS-3/NIST, NRC/SBS-3/USNO and NIST/SBS-3/USNO. The Sagnac corrections are shown in Figure 9, and are indeed small. The variation was less than 20 ps for any one link, and was determined with an accuracy of ± 2 ps. This simple positioning method can evaluate and remove Sagnac effect variations at the ps level.

The satellite position can also affect common-view two-way time transfer measurements by varying the time delay between the two signals each earth station receives: the signal transmitted from the other time laboratory, and the unwanted return signal from its own transmission. The unwanted return signal can pull the timing signal by some 4 ns rms, if the carriers are syntonized. If the rf powers and the modems are matched, the code pullings will almost cancel for the two-way time transfer. However, if there is a 3 dB mismatch in powers (as is commonly observed in our experience) a code pulling of about 1 ns rms can be expected if the carriers are syntonized (for these experiments, they rarely are syntonized within the 2 Hz noise bandwidth of the delay locked loop). The relative delay between the two signals depends mostly on the day-to-day variation in satellite position, the other delays are either constant (equipment delays), slowly varying (the UTC time scale differences) or are settable. During a 300 second timing run, the relative delay may vary by several 400 ns chips as the satellite changes position, but all in a deterministic way. If the two-way time transfer runs are supplemented with a ranging measurement, the effects of code pulling might be evaluated within the limits of our extrapolation accuracy estimate of about 7 ns rms (2% of one chip). The upper bound of the effects of code pulling may be seen in Figures 10 through 13.

In Figure 10, the first difference of the autocorrelation function of Mitrex code 0 (a $[2^{15}-1]$ maximal length PRN code, truncated at 10,000 chips) is shown. The early/late discriminator locks the delay locked loop at the zero crossing of the large negative slope at the origin, of 100% in 400 ns. The details of the autocorrelation function away from the origin are only important in the event of significant multipath signals. In Figures 11 through 13, the first difference of the cross-correlations of the pairs of different Mitrex codes are presented for the ranges of relative delays observed in our experiments with SBS-3. The values on these graphs represent an effective zero-shift for the delay-locked loop, in the case where the unwanted carrier is within the modem's 2 Hz noise bandwidth of the locked carrier. For any particular delay time shown in one of the Figures 11 through 13, the associated code pulling may be read from the graph as a percentage of one chip (400 ns). Also shown for each cross-correlation is a histogram of observed range differences determined in this work. This limit on the size of the code pulling effect can be seen to have been better, by chance, for the NRC/NIST link (Figure 11) than for the USNO/NIST link (Figure 13).

With the Mitrex modems, one interesting possibility is for one station in each transfer to choose its transmit time origin so as to use a part of the cross-correlation that has zero code pulling effect. Of the 28 code pairs that might be used, all but 5 have at least one 400 ns wide range of time delay which has zero code pulling (corresponding to the cross-correlation function having 3 successive values the same). For the Mitrex codes, these flat spots are as follows: code [0,1]: none; [0,2]: 2.396 ms; [0,3]: 3.1876 ms; [0,4]: 0.394, 2.7636 and 3.6984 ms; [0,5]: 0.0472 ms; [0,6]: 0.0536 ms; [0,7]: 0.898 & 0.8984, 2.3388 ms; [1,2]: 0.3184, 0.4932, 1.2652 & 1.2656 ms; [1,3]: 0.650 ms; [1,4]: 0.158, 0.8448 ms; [1,5]: 1.304, 2.6956 ms; [1,6]: none; [1,7]: 3.3936 ms; [2,3]: none; [2,4]: 1.3056, 2.214 ms; [2,5]: 1.5908, 3.6324 ms; [2,6]: 1.9692 ms; [2,7]: none; [3,4]: 0.7332, 3.700 ms; [3,5]: 1.794 ms; [3,6]: 1.0472, 1.1728, 2.6804, 3.9388 ms; [3,7]: 1.144, 3.0832 ms; [4,5]: 0.4708 ms; [4,6]: 1.4304 ms; [4,7]: 0.5784 ms; [5,6]: 0.0972, 2.8724 ms; [5,7]: none; and [6,7]: 0.8576 ms. The crosscorrelation flat spots for [i,j] occur for code i leading or lagging code j by the specified amounts, and the code pulling will then be zero at both earth stations. The times specified with an ampersand (and differing by 400 ns) are flat spots having 4 successive cross correlation values the same, and would be the easiest zero code pulling to use with just a programmable delay generator. The different dopplers would still normally permit 100 s of measurement free from code pulling, but the delay generator would have to be set with 2-station relative position information determined just before the time transfer session (just a few seconds worth of initial measurements, on each of the two codes, taken at only one earth station, would suffice to set the delay generator). As may be seen from the histograms in Figures 11 through 13, the day-to-day position variations do not allow us any confidence to hit even an 800 ns wide window for zero code pulling.

Geostationary satellite position determination by these methods also can make signals from the satellite into useable one-way timing references, with accuracy potential at the 10 ns level, limited principally by the need for position determination at the receiver.

ACKNOWLEDGMENT

The authors wish to thank H.F. Lam for the design and maintenance of the earth station's microwave and electronic equipment.

REFERENCES

1. D.A.Howe, "Stability Measurements of Ku-Band Spread Spectrum Two-Way Time Transfer Equipment", Proc. of the 41st Annual Symposium on Frequency Control, p. 149-160, 1987.
2. D.W.Hanson, "Fundamentals of Two-Way Time Transfers by Satellite", Proc. of the 43rd Annual Symposium on Frequency Control, p. 174-178, 1989.
3. G. de Jong, "Accurate Delay Calibration for Two-way Time Transfer Earth Stations", Proceedings of the 21st Annual Precise Time and Time Interval Applications and Planning Meeting, p. 107-115, 1989.
4. R.N.Treuhhaft, "Tropospheric Limitations to the Stability of Radio Metric Delay Measurements", Proc. of the 21st Annual Precise Time and Time Interval Applications and Planning Meeting, p. 233-238, 1989.
5. Q. Zhuang, et al., "An Investigation of Three Dimension Position Dilution of Precision", Acta Astronomica Sinica, Vol. 32, No. 2, p. 113-120, 1991.

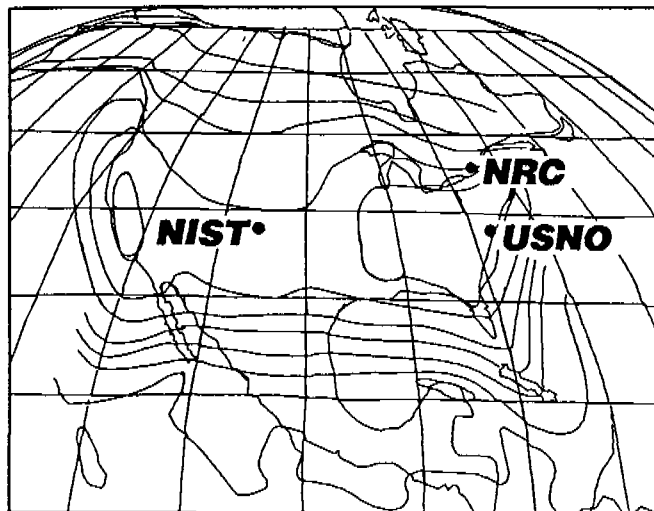


Figure 1. The locations of the time laboratories of NIST, USNO and NRC within the continental beam of SBS-3. The contours are 2 dB apart.

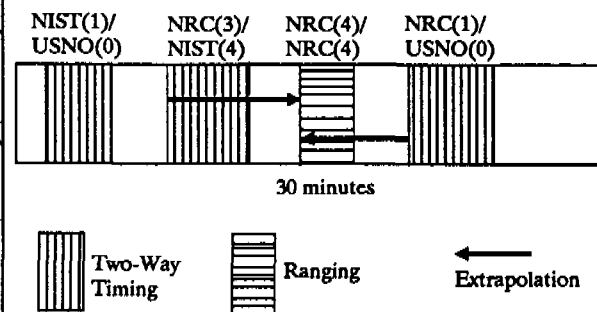


Figure 2. Measurement Schedule for Time Transfer and Ranging.

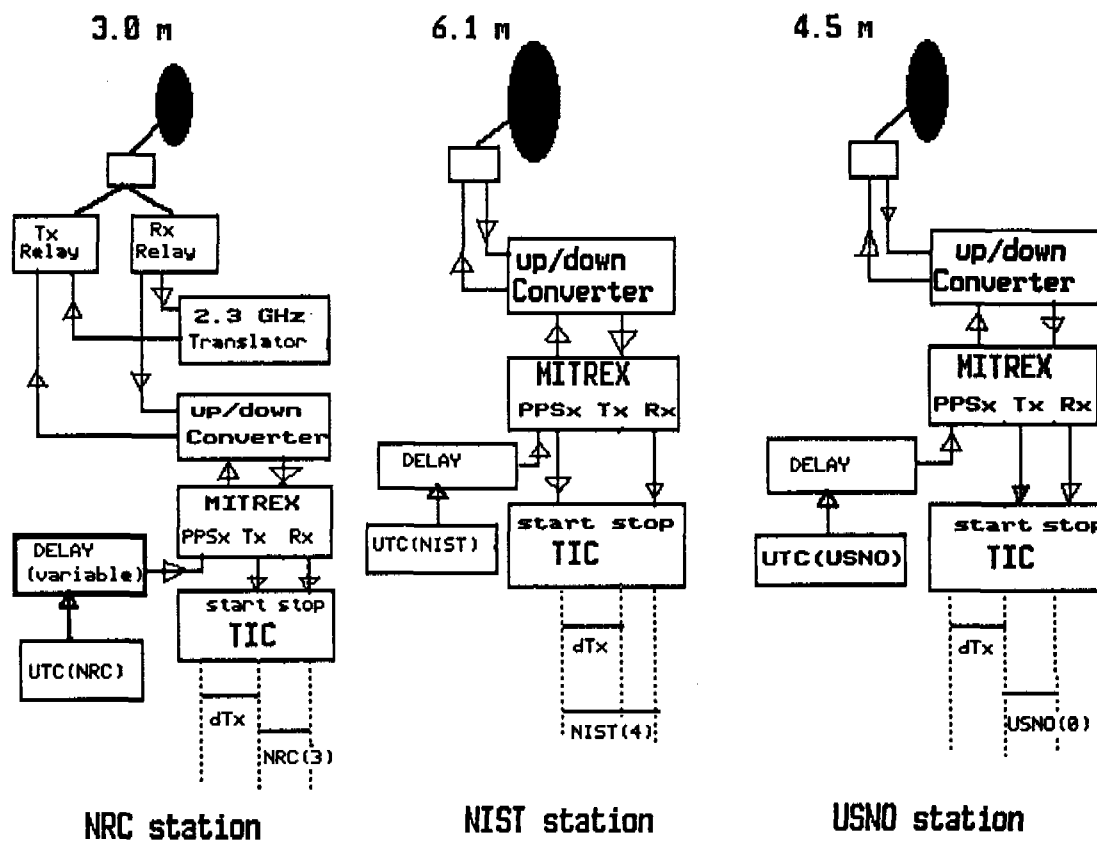


Figure 3. The electronics at the two-way time transfer earth stations at NRC, NIST and USNO.

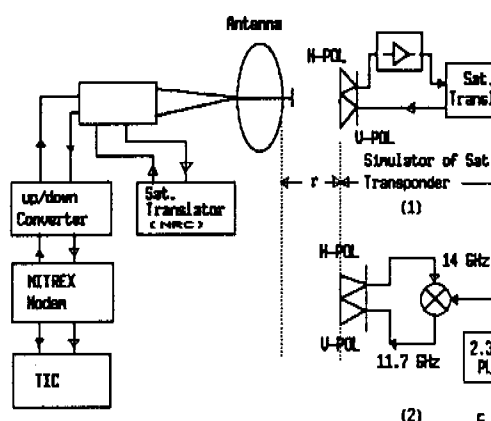


Figure 4. Station Equipment Delay Measurement at NIST (above) and NRC (below).

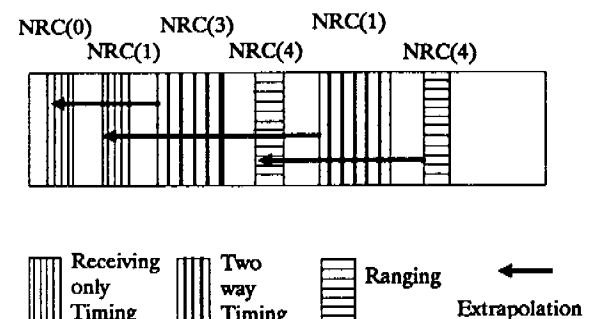


Figure 5. Measurement Schedule for Extrapolation Evaluation

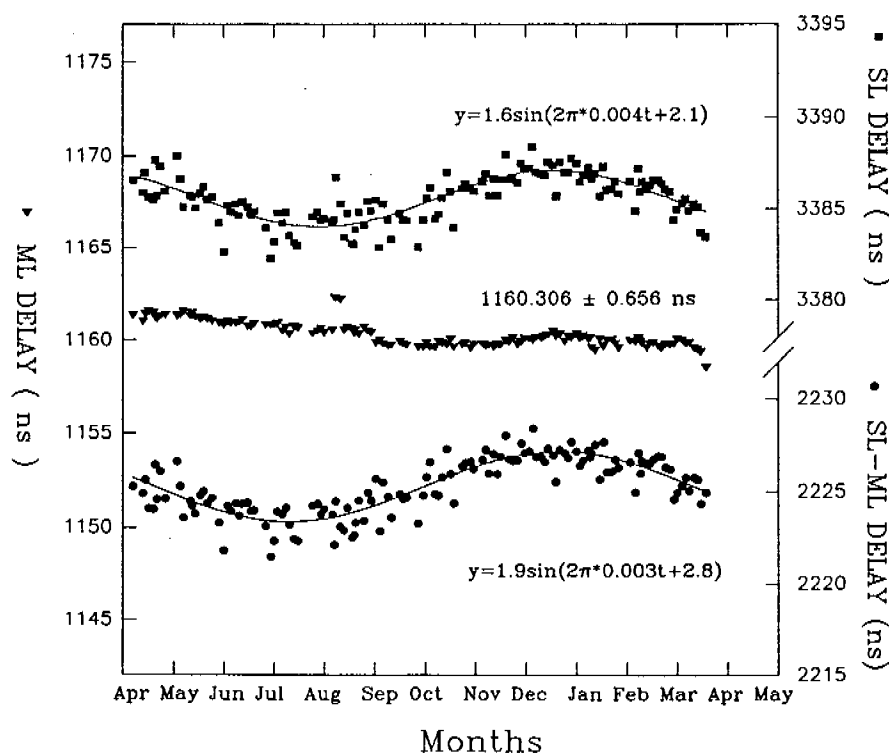


Figure 6. One year's variation of the Mitrex internal modem loop (ML) and the station loop (SL), measured at NRC's earth station.

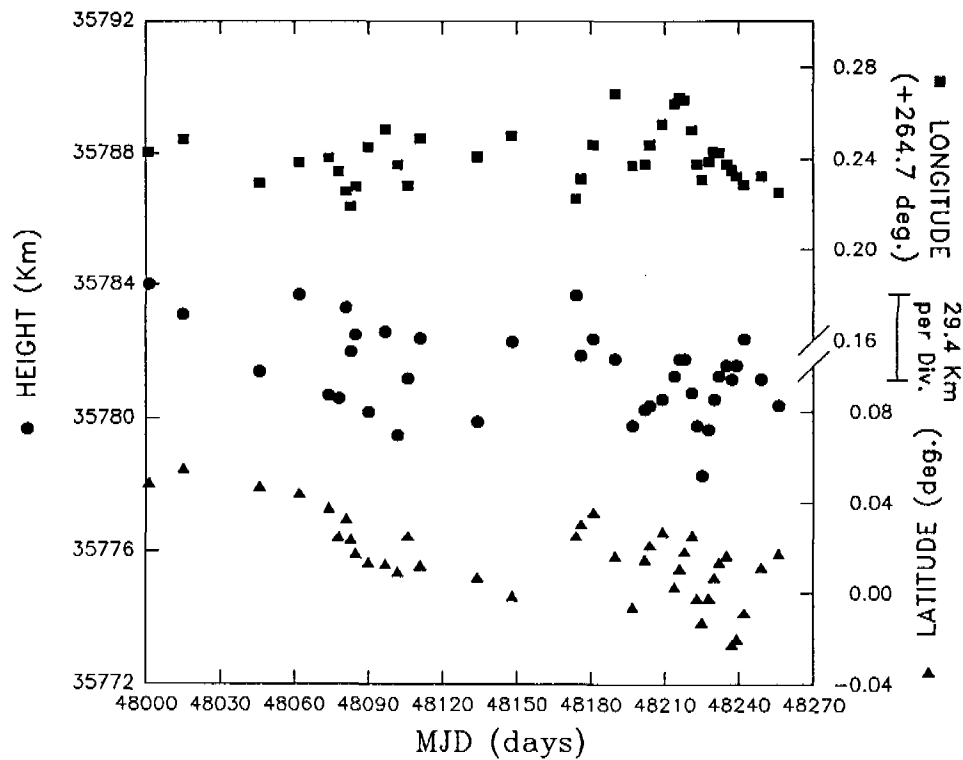


Figure 7. SBS-3 satellite position determination, measured by ranging at NRC and two-way time transfer with NIST and USNO.

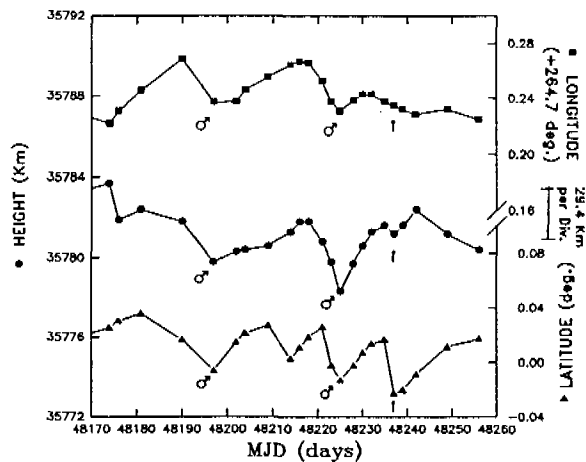


Figure 8. Detail of SBS-3 position determination, illustrating a monthly cycle.

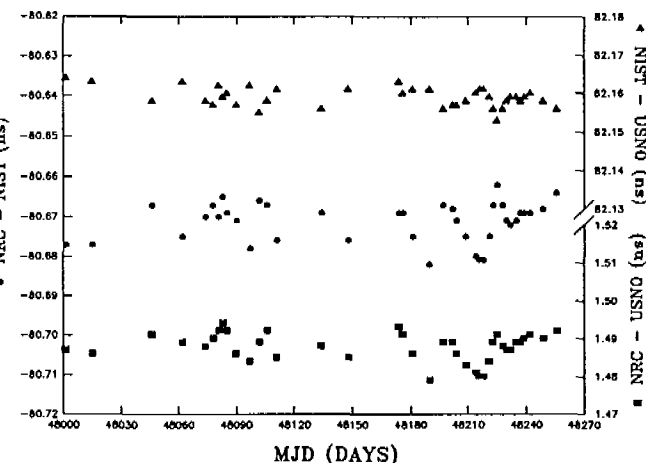


Figure 9. Sagnac effect corrections for links via SBS-3: NRC/NIST (middle); NIST/USNO (top); and NRC/USNO (bottom)- note that although USNO is W of NRC in longitude, it appears E of NRC when viewed from SBS-3.

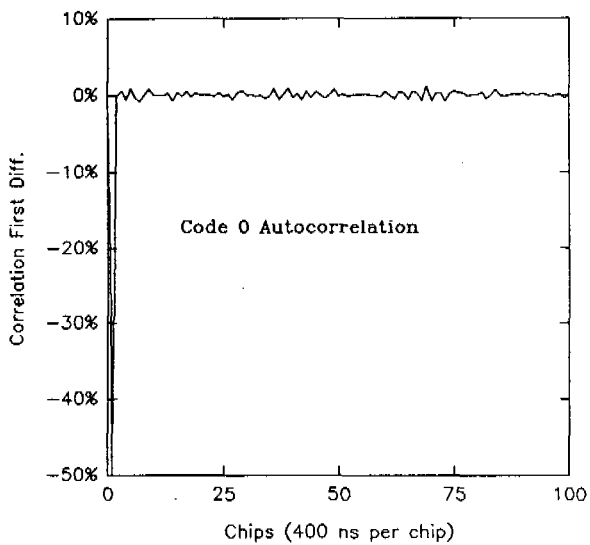


Figure 10. The first difference of the autocorrelation of the Mitrex modem PRN code 0. The vertical scale is normalized to a scale of 100% in 400 ns.

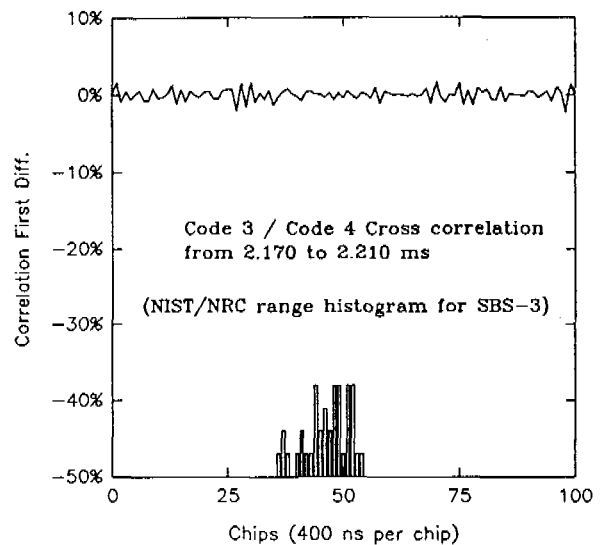


Figure 11. The first difference of the cross correlation of the Mitrex PRN code 3 with code 4, plotted vs relative delay around the NIST/NRC values. Also shown is a histogram of this link's relative delays changed by the position of SBS-3.

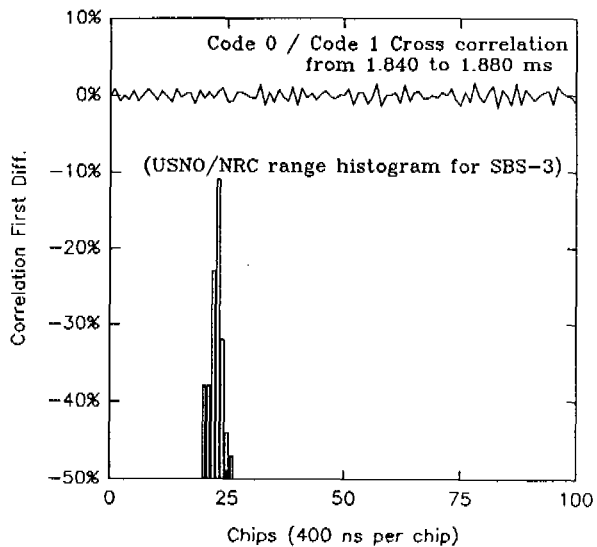


Figure 12. The first difference of the cross correlation of the Mitrex PRN code 0 with code 1, plotted vs relative delay around the USNO/NRC values. Also shown is a histogram of this link's relative delays changed by the position of SBS-3.

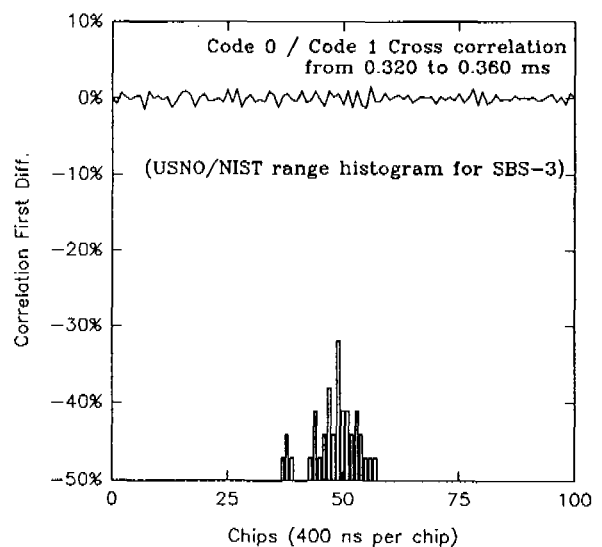


Figure 13. The first difference of the cross correlation of the Mitrex PRN code 0 with code 1, plotted vs relative delay around the USNO/NIST values. Also shown is a histogram of this link's relative delays changed by the position of SBS-3.